Autonomous quantum absorption refrigerators

Sreenath K. Manikandan,[1,2,*] Étienne Jussiau,[1,2,†] and Andrew N. Jordan[1,2,3,‡]

[1]*Department of Physics and Astronomy, University of Rochester, Rochester, New York 14627, USA*
[2]*Center for Coherence and Quantum Optics, University of Rochester, Rochester, New York 14627, USA*
[3]*Institute for Quantum Studies, Chapman University, Orange, California 92866, USA*

(Received 22 October 2020; revised 4 December 2020; accepted 8 December 2020; published 21 December 2020)

We propose a quantum absorption refrigerator using the quantum physics of resonant tunneling through quantum dots. The cold and hot reservoirs are fermionic leads, tunnel coupled via quantum dots to a central fermionic cavity, and we propose configurations in which the heat absorbed from the (very hot) central cavity is used as a resource to selectively transfer heat from the cold reservoir on the left to the hot reservoir on the right. Heat transport in the device is particle-hole symmetric; we find two regimes of cooling as a function of the dot energies—symmetric with respect to the Fermi energy of the reservoirs—and we associate them with heat transfer by electrons above the Fermi level and holes below the Fermi level. We also discuss optimizing the cooling effect by fine-tuning the energy of the dots as well as their linewidth and characterize regimes where the transport is thermodynamically reversible such that the Carnot coefficient of performance is achieved with zero cooling power delivered.

DOI: 10.1103/PhysRevB.102.235427

I. INTRODUCTION

Converting otherwise wasted heat to perform useful work in the nanoscale is an open problem that spans across almost all disciplines of applied science [1–6], including computing [7–12], where there is a lower bound on dissipated heat per cycle of irreversible computation, given by the Landauer's bound [13]. Managing the excess heat generated in circuits is also crucial for various quantum-computing platforms currently available, such as superconducting qubits and matter-based spin qubits, where cooling down to subkelvin temperatures is a must [7]. Besides, efficient cooling below 4 K is a necessity for enhancing the performance of radiation detectors and charge sensors, with benefits also extending to various medical applications, including magnetic resonance imaging [14–16]. Furthermore, subkelvin cooling is essential for exploiting quantum physics in the mesoscopic regime for quantum device applications and for nanoscale energy harvesting with quantum dots [5]. The increasing demand for achieving temperatures nearing absolute zero is largely fulfilled by state-of-the-art dilution refrigerators, which can achieve base temperature down to about 10 mK; even then, localized dissipation of heat remains a major issue to be addressed in places including quantum circuits, where it is a limiting factor for achieving coherent, nonlocal manipulation of quantum information in various quantum-computing platforms currently available [7,17–24].

Cooling has always been an exciting problem in thermodynamics [16], and the advent of quantum technologies presented more recent opportunities for novel refrigeration schemes which can be integrated into various computing platforms and further cool down the devices below ambient temperatures [15]. Some examples of such cooling techniques in the solid state include nuclear demagnetization [16], voltage-biased junction refrigerators [25,26], and Josephson-junction-based refrigerators [27,28] (see also Ref. [15] and references therein). Solid-state refrigeration schemes using adiabatic magnetization of a superconductor have also been proposed, which is particularly useful as a cooling mechanism below the superconducting critical temperatures [29–31].

An alternate approach to dealing with excess heat in quantum circuits is to recycle this heat as a resource to power other quantum thermal machines, such as quantum heat engines and quantum refrigerators [4–6,32–38]. A refrigerator powered by a dissipative heat source is conventionally called an absorption refrigerator [39,40]; the principles of such a cooling technique were known since the 1700s and further developed through the early twentieth century, as an alternative to the standard compression-based refrigerators [41–43]. Albeit having a lower coefficient of performance (COP), the utility of absorption refrigerators emerges from their unique approach to cooling, where excess heat, potentially from a dissipative heat source, is used as a resource to run the cooling cycle. In an evaporation-based absorption refrigeration cycle, the evaporation of a cooling agent at the cold reservoir generates the cooling power. The low vapor pressure required for evaporation is maintained by an absorbing fluid, which reduces the vapor pressure of the cooling agent by absorbing it in the vapor phase. Subsequently, the absorbing agent is heated by an external heat source, which releases the cooling agent, now hotter than its ambient temperature. The excess heat is released into the hot reservoir (typically the environment), and the cooling agent

*skizhakk@ur.rochester.edu
†ejussiau@ur.rochester.edu
‡jordan@pas.rochester.edu

condenses as it flows back into the cold reservoir. The cycle repeats.

Absorption refrigerators that operate at mesoscopic scales, where quantum effects are relevant, have also emerged as one among the prototypical systems to probe thermodynamics in the quantum regime [38,44–48]. A canonical model would consist of three reservoirs—cold (L), hot (R), and hotter (H), where $T_L < T_R < T_H$—and quantum systems (possibly qubits) interacting among themselves, as well as with the reservoirs. The interactions are such that the spontaneous flow of heat in the direction H $\rightarrow$ R also induces a flow of heat in the direction L $\rightarrow$ R, resulting in further cooling of the reservoir L. See, for instance, Ref. [49], where a proposal for such an absorption refrigerator using Coulomb-coupled quantum dots or metallic islands is discussed. It has also been pointed out that quantum coherent effects may enhance the performance of absorption refrigerators in the quantum regime [50,51], suggesting that absorption refrigerators may be used to probe quantum advantages in the operation of thermal machines.

Thermoelectric effects in nanoscale devices are tightly linked to their energy-filtering properties [52]. Allowing a flow of electrons between two terminals at certain energies only can give rise to a flow of charge against an electrochemical potential or a flow of heat against a temperature bias. A thermoelectric device is then characterized by its transmission function $\mathcal{T}(E)$ describing the probability for an electron at energy E to traverse the system. Typically, thermoelectric effects arise in devices for which $\mathcal{T}(E)$ behaves differently above and below the Fermi energy [38]. We then understand the importance of working with devices with prominent and well-characterized energy-filtering properties. This is why many experimental realizations of nanoscale thermoelectrics make use of quantum dots whose transmission function is given by a Lorentzian function centered at the resonant dot energy [48,53–55].

In this paper, we propose a quantum absorption refrigerator where we take advantage of the quantum physics of resonant tunneling through quantum dots to achieve the unidirectional flow of heat required for refrigeration. In our proposal, we consider an energy-filtering configuration for the dot energies, similar to the one considered in Refs. [35,37]. We present an experimentally viable design motivated by a recently realized energy-harvesting quantum device discussed in Ref. [48].

The configuration we consider is sketched in Fig. 1. The reservoir H is a fermionic cavity that is coupled to a cold reservoir L on the left and a hot reservoir R on the right via quantum dots having prescribed energies. Refrigerator configurations in such architectures have been investigated in Refs. [53,56], where the goal is to cool down the central cavity, H. A variant of this, where quantum dots are replaced by superlattices, is presented in Ref. [57]. Similar tunnel coupling to cool down a central metallic reservoir using selective transfer of hot electrons and holes to left and right reservoirs has also been proposed [58]. In contrast, our present study investigates whether it is possible to think of the fermionic cavity as a hot spot in a circuit, which allows us to extract finite cooling power from the cold reservoir L. In addition to that, we also provide a complete thermodynamic characterization of the device and discuss its optimal and stopping

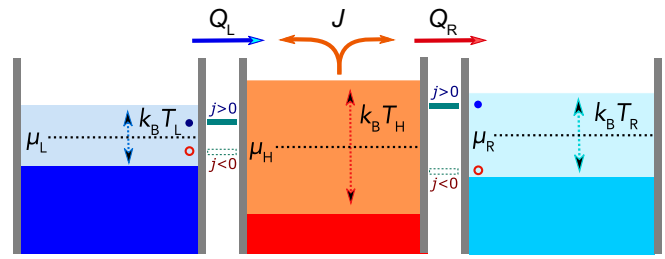

FIG. 1. Schematic of the particle current j and heat currents Q_L, Q_R, and J in the absorption refrigerator. The bias of the dot energies E_L and E_R with respect to the Fermi energy of the leads chooses whether the transport is mediated by electrons (above the Fermi energy of the leads, $j > 0$) or holes (below the Fermi energy of the leads, $j < 0$). Nevertheless, the heat currents are invariant under this choice of bias, depicting particle-hole symmetry in the transport problem.

configurations. Our analysis also makes simple connections to the particle-hole symmetry in the transport problem from a thermodynamic point of view, which reveals two equivalent bias configurations for the operation of our absorption refrigerator. They correspond to the energy of the dots positioned above the Fermi level (mediated by hot electrons) and below the Fermi level (mediated by hot holes), respectively.

Note that a pedagogical analogy can be made to a conventional refrigerator context, where work has to be supplied to refrigerate reservoir L relative to reservoir R. Here, one can think of reservoirs H and R as analogous to the hot and cold reservoirs of an engine, which supply the necessary work required for cooling in a conventional refrigerator, where the heat flow in the direction H $\rightarrow$ R generates the fiducial work to run the refrigeration of reservoir L relative to reservoir R.

In the discussions which follow, we provide a systematic characterization of our quantum absorption refrigerator in its steady state. The system obeys both particle and energy current conservation laws in the steady state. We further assume that the chemical potentials are identical for reservoirs L and R, so as to ensure that our device qualifies as an absorption refrigerator. Indeed, in such a situation, the refrigeration is solely powered by the heat provided by the hot cavity H, contrary to standard nanoscale refrigerators where a voltage bias enables electric power generation to fuel the refrigerator [15,26]. From the point of view of electrons leaving the cold reservoir, they have to gain definite energy from cavity H to overcome the temperature difference and exit to the hot reservoir on the right. However, we can add a voltage bias to our setup to design hybrid devices that use the heat from the cavity both to cool down reservoir L and generate electric power in reservoir R (if $\mu_L < \mu_R$), or conversely, we can imagine a "doped" absorption refrigerator whose performance is improved using electric power alongside the heat from the cavity (if $\mu_L > \mu_R$).

A crucial assumption we make is that the hot and cold reservoirs are connected to some external circuit, while the cavity is in thermal equilibrium with a separate heat reservoir. As such, reservoirs L and R can exchange particles with their environment, and their chemical potentials μ_L and μ_R can then be imposed externally. On the contrary, the number of

particles in the cavity is constant, and its chemical potential is then fixed by particle conservation [59]. Furthermore, we assume that strong inelastic electron-electron or electron-phonon interactions taking place in the cavity cause electrons entering it to relax on a time scale much shorter than the time they will spend there. As such, electron populations in the cavity are described by the usual Fermi factors, where the chemical potential is determined through particle conservation.

In this paper, we focus on the situation where the device operates as a steady-state absorption refrigerator and thus assume that all its characteristic parameters (temperatures, dot energies, and chemical potentials) are constant in time. The steady-state behavior of the machine is described using the Landauer-Büttiker scattering theory [38,60–63]. This formalism can be straightforwardly extended to situations with time-varying parameters when these variations are much slower than the typical time necessary for electrons to traverse the system. In this so-called adiabatic limit, electrons do not feel the change in the device properties, and the time-dependent problem is then treated by simply reusing the results derived in the time-independent case, albeit with time-dependent parameters [64–66]. Sophisticated techniques have been developed to address the case of nonadiabatically varying parameters [4,66], where the information obtained in the stationary case no longer suffices to solve the problem. For the setup studied here, not only the dwell time for electrons in the dots must be taken into account, but also the thermalization time for electrons in the cavity. Indeed, if the parameters of the problem were to vary on a time scale shorter or comparable to this relaxation time, a nonequilibrium distribution of electrons in the cavity would arise instead of the Fermi-Dirac distribution considered hereafter. Such considerations are outside the scope of this work.

This paper is organized as follows. We first discuss our model in detail, in light of the conservation laws. We then extend this discussion to characterize the laws of thermodynamics for our absorption refrigerator, assuming vanishing linewidth for the quantum dots. In subsequent sections we prescribe methods to optimize cooling power over energy of the dots, as well as temperature of the leads involved. We also numerically investigate optimizing the cooling power over the finite linewidth of the quantum dots and present estimates of experimentally achievable figures of merit for our quantum absorption refrigerator.

II. THE MODEL AND CONSERVATION LAWS

We consider two fermionic reservoirs L and R connected via two quantum dots at energies $E_{\rm L}$ and $E_{\rm R}$ to a cavity H in the middle (see Fig. 1). The resonant-tunneling quantum dots are tunnel coupled to the reservoirs and cavity, each contact being characterized by a tunneling rate γ_α which corresponds to the inverse lifetime of an electron on the dot and is also referred to as the level width for the dot. In what follows, we will assume symmetric coupling; that is, all tunnel rates are taken to be equal, $\gamma_{\rm L} = \gamma_{\rm R} = \gamma$.

Electron populations in the leads and cavity are described by the Fermi-Dirac distributions

$$f(E-\mu_\alpha, T_\alpha) = (e^{\frac{E-\mu_\alpha}{k_{\rm B}T_\alpha}}+1)^{-1}, \quad \alpha = {\rm L, R, H}. \tag{1}$$

Here, μ_α are the chemical potential of reservoir α, and $k_{\rm B}$ is the Boltzmann's constant. The particle and energy currents out of reservoir $\alpha = {\rm L, R}$, denoted by j_α and J_α, respectively, are given by the Landauer-Büttiker-type expressions [38,60–63]

$$j_\alpha = \frac{2}{h}\int dE\, \mathcal{T}_\alpha(E)[f(E-\mu_\alpha, T_\alpha) - f(E-\mu_{\rm H}, T_{\rm H})], \tag{2}$$

$$J_\alpha = \frac{2}{h}\int dE\, E\mathcal{T}_\alpha(E)[f(E-\mu_\alpha, T_\alpha) - f(E-\mu_{\rm H}, T_{\rm H})], \tag{3}$$

where $\mathcal{T}_\alpha(E)$, the transmission function for dot α, assumes a Lorentzian shape for resonant tunneling [38,63],

$$\mathcal{T}_\alpha(E) = \frac{\gamma^2}{(E-E_\alpha)^2+\gamma^2}. \tag{4}$$

We furthermore define the heat current associated with each of the leads as

$$Q_\alpha = J_\alpha - \mu_\alpha j_\alpha. \tag{5}$$

The chemical potential of the cavity cannot be chosen arbitrarily; it is constrained by particle conservation across the device,

$$j_{\rm L} + j_{\rm R} = 0. \tag{6}$$

The above relation clearly asserts that the net particle current out of the cavity vanishes in the steady state. Consequently, the total heat current J flowing out the cavity coincides with the corresponding energy current [35] and can thus be inferred from energy conservation,

$$J + J_{\rm L} + J_{\rm R} = 0. \tag{7}$$

J is identified as the heat current driving the absorption refrigerator.

In general, the conservation laws in Eqs. (6) and (7) cannot be solved exactly. It is, however, possible in the narrow-linewidth regime, $\gamma \ll k_{\rm B}T_{\rm L}, k_{\rm B}T_{\rm R}, k_{\rm B}T_{\rm H}$, where the transmission function in Eq. (4) can be approximated by $\mathcal{T}_\alpha(E) = \pi\gamma\delta(E-E_\alpha)$ owing to the δ-function limit of the Lorentzian function,

$$\lim_{\gamma\to 0}\frac{\gamma}{x^2+\gamma^2} = \pi\delta(x). \tag{8}$$

In this regime, the conservation equations become

$$f(E_{\rm L}-\mu_{\rm L}, T_{\rm L}) - f(E_{\rm L}-\mu_{\rm H}, T_{\rm H}) + f(E_{\rm R}-\mu_{\rm R}, T_{\rm R}) - f(E_{\rm R}-\mu_{\rm H}, T_{\rm H}) = 0, \tag{9}$$

$$J + \frac{\gamma E_{\rm L}}{\hbar}[f(E_{\rm L}-\mu_{\rm L}, T_{\rm L}) - f(E_{\rm L}-\mu_{\rm H}, T_{\rm H})] + \frac{\gamma E_{\rm R}}{\hbar}[f(E_{\rm R}-\mu_{\rm R}, T_{\rm R}) - f(E_{\rm R}-\mu_{\rm H}, T_{\rm H})] = 0, \tag{10}$$

reminiscent of similar equations in Ref. [35]. Above, Eq. (9) suggests that the parameters in the transport problem cannot be defined independently of each other as a result of current conservation. We can therefore use Eq. (9) to determine the chemical potential of the cavity $\mu_{\rm H}$ as a function of other parameters, such as the energy of the dots and chemical potential of the external leads, $\mu_{\rm L}$ and $\mu_{\rm R}$ (see Appendix A). This is because these parameters—the energy of the dots and the chemical potential of the external leads—are typically fixed in a given experimental setting, which can be controlled via external voltage controls.

Solving Eq. (9) for the chemical potential $\mu_{\rm H}$ yields an exact expression for the particle current across the device,

$$\begin{aligned} j &= \frac{\gamma}{\hbar}[f(E_{\rm L}-\mu_{\rm L},T_{\rm L})-f(E_{\rm L}-\mu_{\rm H},T_{\rm H})] \\ &= \frac{\gamma}{\hbar}[f(E_{\rm R}-\mu_{\rm H},T_{\rm H})-f(E_{\rm R}-\mu_{\rm R},T_{\rm R})]. \end{aligned} \tag{11}$$

The heat current J then straightforwardly follows: From Eq. (10), we find $J = j\Delta E$, where $\Delta E = E_{\rm R} - E_{\rm L}$ is the energy gain between the right and left dots. Such a relation is typical of the so-called tight-coupling limit, where particle and energy currents are proportional to one another. Indeed, in the narrow-linewidth limit, each electron flowing from L to R necessarily carries a definite amount ΔE of energy. This property no longer holds when γ increases as the dots' energy levels widen allowing electrons with different energies to pass.

III. THERMODYNAMIC ANALYSIS

A. Thermodynamics of the absorption refrigerator

We now analyze the situation where the device is used as an absorption refrigerator and characterize it thermodynamically. We want to use the heat from the hottest cavity as a resource to induce a heat current out of the coldest reservoir without electrical power being involved. Here, we assume $T_{\rm L} < T_{\rm R} < T_{\rm H}$ and $\mu_{\rm L} = \mu_{\rm R} = \mu$. Hereafter, we set the zero of energy at μ without loss of generality. Furthermore, for the system to function as a refrigerator, the cooling power, which is the heat current out of the cold reservoir, must be positive, namely, $Q_{\rm L} > 0$. For the device at stake here, the laws of thermodynamics read

$$J + Q_{\rm L} + Q_{\rm R} = 0, \tag{12}$$

which is the statement of global conservation of energy (first law), and (the second law of thermodynamics in the Clausius form [67])

$$\frac{J}{T_{\rm H}} + \frac{Q_{\rm L}}{T_{\rm L}} + \frac{Q_{\rm R}}{T_{\rm R}} \leqslant 0. \tag{13}$$

The first law of thermodynamics in Eq. (12) enables us to eliminate one of the heat currents from the entropy balance in Eq. (13). As such, we obtain

$$J\left(\frac{1}{T_{\rm R}}-\frac{1}{T_{\rm H}}\right) \geqslant Q_{\rm L}\left(\frac{1}{T_{\rm L}}-\frac{1}{T_{\rm R}}\right) \geqslant 0 \tag{14}$$

and

$$Q_{\rm R}\left(\frac{1}{T_{\rm H}}-\frac{1}{T_{\rm R}}\right) \geqslant Q_{\rm L}\left(\frac{1}{T_{\rm L}}-\frac{1}{T_{\rm H}}\right) \geqslant 0. \tag{15}$$

Our choice $T_{\rm H} > T_{\rm R}$ imposes $J \geqslant 0$, and $Q_{\rm R} \leqslant 0$. In this situation, the heat out of the cavity H drives a heat current from reservoir L to reservoir R, enabling cooling of the former. The COP of the absorption refrigerator is then defined as

$$C = \frac{Q_{\rm L}}{J}. \tag{16}$$

The COP is maximum when the refrigerators operates reversibly. We refer to this upper bound as the Carnot COP, and its value can be obtained from Eq. (14),

$$\begin{aligned} &J\left(\frac{1}{T_{\rm R}}-\frac{1}{T_{\rm H}}\right) \geqslant Q_{\rm L}\left(\frac{1}{T_{\rm L}}-\frac{1}{T_{\rm R}}\right) \\ &\Rightarrow C = \frac{Q_{\rm L}}{J} \leqslant \frac{T_{\rm R}^{-1}-T_{\rm H}^{-1}}{T_{\rm L}^{-1}-T_{\rm R}^{-1}} = C_{\rm Carnot}. \end{aligned} \tag{17}$$

B. Vanishingly small linewidth

These thermodynamic relations can be written in terms of the microscopic details of our device in the limit of small level width, $\gamma \ll k_{\rm B}T_{\rm L}$. In this regime, we have $Q_{\rm L} = jE_{\rm L}$, $Q_{\rm R} = -jE_{\rm R}$, and $J = j\Delta E$. The second law in Eq. (13) then becomes

$$j\left(\frac{\Delta E}{T_{\rm H}}+\frac{E_{\rm L}}{T_{\rm L}}-\frac{E_{\rm R}}{T_{\rm R}}\right) \leqslant 0, \tag{18}$$

and the COP is given by

$$C = \frac{E_{\rm L}}{\Delta E}. \tag{19}$$

Interestingly, there are two possible choices for the relative positions of the dot energies and Fermi level such that $J \geqslant 0$, $Q_{\rm L} \geqslant 0$, and $Q_{\rm R} \leqslant 0$. In comparison to the electric-current-rectification case discussed in Ref. [35], where the dot energies are positioned above and below the Fermi energy, here both the dot energies are positioned either above or below the Fermi energy. They respectively correspond to $E_{\rm R} > E_{\rm L} > 0$, where the particle current flows from L to R ($j > 0$), or $E_{\rm R} < E_{\rm L} < 0$, where the particle current flows from R to L ($j < 0$). In the former case, hot electrons are taken out of the cold reservoir, while cold electrons are injected into the cold reservoir in the latter case. Alternatively, the latter case can be viewed as the transport of hot holes below the Fermi energy (taken as the zero of energy); see Fig. 1. We note that this is a manifestation of particle-hole symmetry in the underlying transport problem, which is often an overlooked aspect but has interesting consequences; in our absorption refrigerator context, the particle-hole symmetry can be exploited as an additional freedom of choice for the biasing of dot energies relative to the Fermi energy, and this freedom could be beneficial in an experimental implementation of our proposal.

The thermodynamic analysis presented above allows us to predict the temperature of the hot reservoir R for which cooling power vanishes. According to Eq. (18), for $j > 0$, we must have

$$\frac{E_{\rm L}}{T_{\rm L}} - \frac{E_{\rm R}}{T_{\rm R}} + \frac{\Delta E}{T_{\rm H}} \leqslant 0, \tag{20}$$

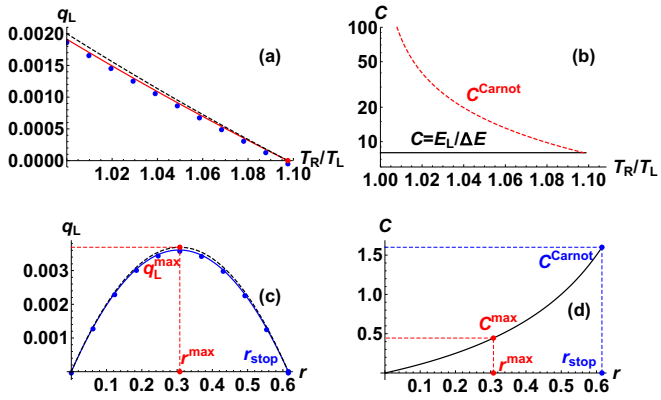

FIG. 2. (a) The cooling power Q_L in dimensionless units, $q_L = \hbar Q_L/(\gamma k_B T_L)$, as a function of T_R/T_L. We also compare the numerical calculation for q_L for small, but finite, linewidth (blue dots) with exact predictions assuming a δ transmission function (red solid curve), as well as linear response regime results (black dashed curve). We choose $\mu_L = \mu_R = 0$, $T_H = 5T_L$, $E_L = 0.4k_B T_L$, $E_R = 0.45k_B T_L$, and $\gamma = 10^{-4}k_B T_L$. (b) COP C as a function of T_R/T_L. Note that Carnot COP is reached at $T_R = T_{stop}$. (c) Comparing the numerical calculation for q_L for small, but finite, linewidth (blue dots) with exact predictions assuming a δ transmission function (blue solid curve), as well as linear response regime results (black dashed curve) for different values of $r = E_L/E_R$. We choose $\mu_L = \mu_R = 0$, $T_R = 1.5T_L$, $T_H = 5T_R$, $E_R = 0.6k_B T_L$, and $\gamma = 10^{-4}E_R$. (d) COP of the absorption refrigerator. It is shown that the refrigerator achieves Carnot COP at the stopping energy, $E_L = r_{stop}E_R$, and that the coefficient of performance at E_L^{max} is $C^{max} = (T_R^{-1} - T_H^{-1})/(2T_L^{-1} - T_R^{-1} - T_H^{-1})$.

while, for $j < 0$, we must have

$$\frac{E_L}{T_L} - \frac{E_R}{T_R} + \frac{\Delta E}{T_H} \geqslant 0. \tag{21}$$

In either of the cases the stopping configuration corresponds to saturating the equality in Eqs. (20) and (21), as the entropy change becomes zero and the system becomes thermodynamically reversible. Solving for $T_R = T_{stop}$, we obtain

$$T_{stop} = E_R\left(\frac{E_L}{T_L} + \frac{\Delta E}{T_H}\right)^{-1}. \tag{22}$$

The cooling power drops to zero at $T_R = T_{stop}$, as demonstrated in Fig. 2(a). This hints at the fact that the transport of electrons is thermodynamically reversible at the stopping configuration. This can be straightforwardly verified by showing that Carnot COP is achieved in this situation; see Fig. 2(b).

IV. OPTIMIZING THE COOLING POWER

In this section, we discuss systematically optimizing the performance of our absorption refrigerator. We focus on the parameters which can be tuned via external control, such as the energy of the dots, as well as their linewidth. We compute their optimal values numerically and compare with exact analytical predictions whenever possible.

A. Optimizing with respect to the dot energies

We first discuss the optimal and stopping configurations with respect to varying the energy of the left dot when all other parameters are assumed to have fixed values. We further assume that we are in the limit of vanishing level width, $\gamma \ll k_B T_L$. Hereafter, we assume $j > 0$, such that $E_R > E_L > 0$ according to Eq. (18). In this regime, the second law implies

$$E_L\left(\frac{1}{T_L} - \frac{1}{T_H}\right) \leqslant E_R\left(\frac{1}{T_R} - \frac{1}{T_H}\right). \tag{23}$$

We deduce that the system operates as an absorption refrigerator if the dot energies satisfy

$$0 \leqslant E_L \leqslant r_{stop}E_R, \tag{24}$$

where we have introduced the stopping ratio

$$r_{stop} = \frac{T_R^{-1} - T_H^{-1}}{T_L^{-1} - T_H^{-1}}. \tag{25}$$

The cooling power goes to zero at this stopping configuration where electron transport is thermodynamically reversible and thus achieves Carnot COP. This is demonstrated in Figs. 2(c) and 2(d), respectively.

We now discuss the optimal point of operation of the refrigerator by first solving for the chemical potential of the reservoir μ_H (see Appendix A) and then optimizing the cooling power Q_L with respect to the energy of the left dot. However, the solution for μ_H does not allow for further analytical calculations in the general case, and additional approximations are necessary. In what follows, we will assume that the energy differences between dot energies and chemical potentials are small, so that the Fermi factors can be expanded as follows:

$$f(E - \mu, T) \approx \frac{1}{2} - \frac{E - \mu}{4k_B T}. \tag{26}$$

Such simplification is accurate for $|E - \mu| \ll k_B T$ [68]. In this regime, the cavity chemical potential is given by

$$\mu_H \approx -\frac{E_L}{2}\left(\frac{T_H}{T_L} - 1\right) - \frac{E_R}{2}\left(\frac{T_H}{T_R} - 1\right). \tag{27}$$

The cooling power then reads

$$Q_L = \frac{\gamma E_L}{8\hbar k_B T_H}\left[E_R\left(\frac{T_H}{T_R} - 1\right) - E_L\left(\frac{T_H}{T_L} - 1\right)\right]. \tag{28}$$

We find that cooling power is maximum when the left-dot energy is precisely at the center of its allowed range, $E_L^{max} = r_{stop}E_R/2$, where

$$Q_L^{max} = \frac{\gamma E_R^2\left(T_R^{-1} - T_H^{-1}\right)^2}{32\hbar k_B\left(T_L^{-1} - T_H^{-1}\right)}. \tag{29}$$

The corresponding COP is

$$C^{max} = \frac{T_R^{-1} - T_H^{-1}}{2T_L^{-1} - T_R^{-1} - T_H^{-1}}. \tag{30}$$

We indicate these optimal configurations in Figs. 2(c) and 2(d). Further optimization of the device by varying more than one parameter at once is shown in Figs. 3 and 4.

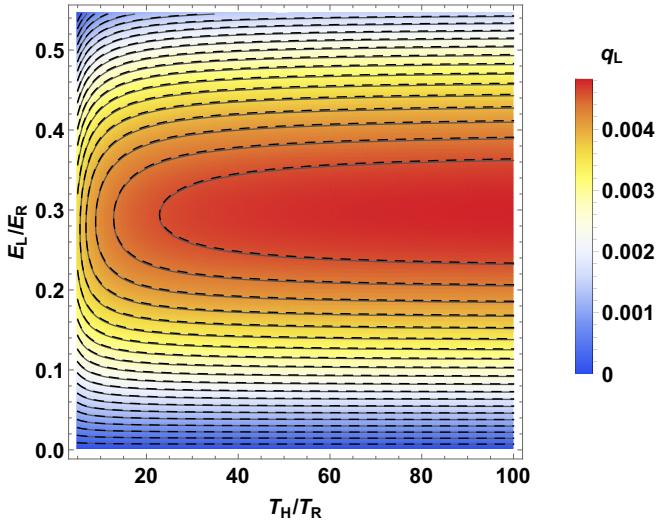

FIG. 3. The cooling power Q_L in dimensionless units, $q_L = \hbar Q_L/(\gamma k_B T_L)$, as a function of dot energies, as well as temperatures. The contour lines are obtained independently in the small-linewidth limit from exact calculations (solid curves) and linear response results (dashed curves). We choose $\mu_L = \mu_R = 0$, $T_L = 0.6T_R$, and $E_R = 0.4k_B T_R$. The minimum temperature of reservoir H is set at $T_H = 5T_R$, and the maximum value of the ratio E_L/E_R is taken to be the stopping ratio r_{stop} for this minimum temperature.

Analogous to the rectification of a current without any voltage difference [35], we note from Eq. (28) that it is possible to drive a rectified heat current even if there is no thermal bias between reservoirs L and R, $T_L = T_R = T$. In this case the heat current out of reservoir L is given by

$$Q_L = \frac{\gamma E_L \Delta E}{8\hbar k_B T_H}\left(\frac{T_H}{T} - 1\right). \tag{31}$$

In this situation, the direction of the heat flow, along with the direction of the particle current, is entirely then determined by the relative position of the dot energies. For example, let us consider a setup with $E_L > 0$ and $E_R > 0$, in which case heat transport is mediated by hot electrons; we have $Q_L > 0$ ($j > 0$) if $E_R > E_L$, while $Q_R > 0$ ($j < 0$) if $E_R < E_L$. More details about this rectified heat current are given in Appendix B.

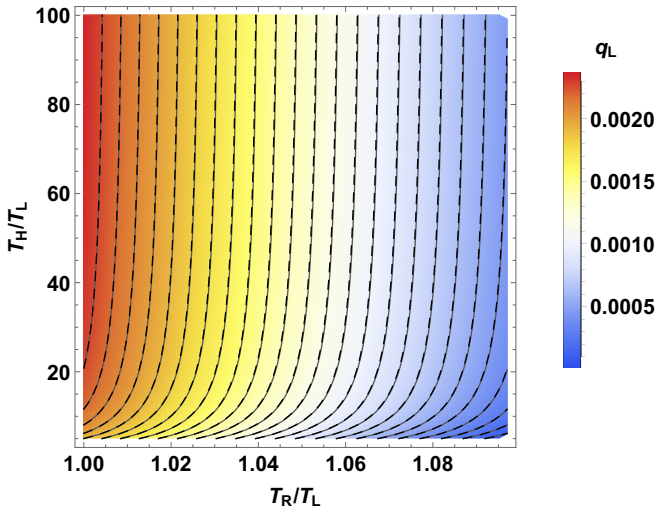

FIG. 4. The cooling power Q_L in dimensionless units, $q_L = \hbar Q_L/(\gamma k_B T_L)$, as a function of the different temperatures involved. The contour lines are obtained independently in the small-linewidth limit from exact calculations (solid curves) and linear response results (dashed curves). We choose $\mu_L = \mu_R = 0$, $E_L = 0.4k_B T_L$, and $E_R = 0.45k_B T_L$. The maximum value of the temperature T_R is taken to be the stopping temperature T_{stop} calculated when the temperature takes its minimum value $T_H = 5T_L$.

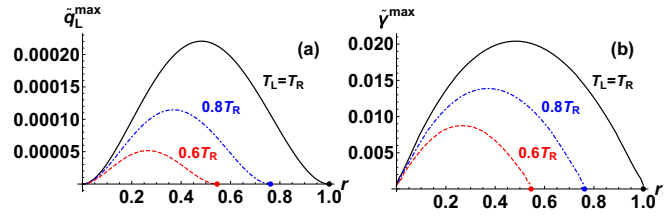

FIG. 5. Optimization over finite linewidth. We perform exact numerical simulation of the integrals involved where the energy of the dots and temperatures are not restricted to the regime of validity of linear response theory. (a) The maximum cooling power Q_L^{max} in dimensionless units, $\tilde{q}_L^{max} = \hbar Q_L^{max}/(k_B T_R)^2$, as a function of the energy ratio r for different values of T_L. We choose $\mu_L = \mu_R = 0$, $T_H = 5T_R$, $E_R = k_B T_R$, and $\gamma = \gamma^{max}(rE_R, E_R, T_L, T_R, T_H)$. (b) The maximum cooling-power linewidth $\gamma = \gamma^{max}(rE_R, E_R, T_L, T_R, T_H)$ in dimensionless units, $\tilde{\gamma}^{max} = \gamma^{max}/k_B T_R$, is shown as a function of r. The stopping values of r are shown as dots, and they correspond to the values obtained assuming vanishing linewidth. The $T_L = T_R$ case corresponds to the rectification configuration discussed in Appendix B.

B. Optimizing with respect to the linewidth γ

We now generalize our discussion to finite linewidth γ characterizing the transmission through the dots. The linewidth γ is an additional important parameter which can be optimized to our advantage in a realistic experiment. Physically, as we increase the linewidth, electrons from a wider range of energy can participate in the transport process. However, soon the cooling power tends to drop with further increase in the linewidth because increasing the linewidth above a threshold reduces the energy-filtering effect necessary for the operation of our absorption refrigeration scheme. Therefore there is an optimal linewidth $\gamma = \gamma^{max}$ which will depend on the energy of the dots as well as the temperature of the leads. We compute γ^{max} numerically. We demonstrate this optimization in Fig. 5(a), where each point in the curve corresponds to an optimization over the linewidth γ. The optimal γ which maximizes the cooling power for each value of r is shown in Fig. 5(b). We observe that the allowed range of values for the left-dot energies shrinks (from above and below) as the level width is increased. Interestingly, there is a critical level width above which refrigeration becomes impossible. Our numerical results further substantiate our choice to work in the regime of vanishingly small level width since we find that γ^{max} is typically one or two orders of magnitude smaller

than the temperature. This is in stark contrast with Ref. [35], where the same device is used as an energy harvester. There, the optimal level width for electric power generation is found to be of the order of the temperature of the leads. This substantial difference is seemingly due to the different positions of dot energies: In Ref. [35], dot energies are symmetrically placed with respect to the average chemical potential of the leads, while here, we have argued that refrigeration can only be achieved if both dot energies are above (or below) the common chemical potential of the leads (taken as the zero of energy throughout our analysis).

Numerically analyzing the particle and energy currents as functions of the linewidth γ, we find that their large-scale variations with γ do not strongly depend on the dot energies. As already noted in Ref. [35], the particle current [69] first increases with γ, reaching a maximum for $\gamma \sim k_B T_L$, but it then decreases, approaching zero as γ becomes larger. The heat current typically decreases with γ and plateaus at $Q_L = -\pi^2 k_B^2 (T_H^2 - T_L^2)/(3h)$ for relatively large linewidths, $\gamma \gtrsim 10 k_B T_L$. More details about the behavior of currents for large γ are given in Appendix C. Our numerics indicate that we must restrict ourselves to cases where $\gamma \ll k_B T_L$. More precisely, we find that the only cases where the device can operate as a refrigerator are those where the heat current first increases with γ but then decreases after having reached a maximum for $\gamma = \gamma^{\max}$. The possibility to use the device as a refrigerator will then be determined by its behavior for small γ, which is obtained using the limit in Eq. (8) and has been extensively studied in this paper. We have found that $Q_L \approx \gamma \hbar^{-1} E_L [f(E_L, T_L) - f(E_L - \mu_H, T_H)]$ for $\gamma \ll k_B T_L$, which means that the possibility for refrigeration at *any* value of γ will be determined by the sign of the initial slope $\hbar^{-1} E_L [f(E_L, T_L) - f(E_L - \mu_H, T_H)]$, refrigeration being possible only if it is positive. Interestingly, we note that the sign of this quantity has already been analyzed in Eq. (18), which is simply a restatement of the second law of thermodynamics in the limit $\gamma \ll k_B T_L$. The possibility for our device to operate as a refrigerator is thus entirely determined by the fundamental laws of thermodynamics expressed in the limiting case of vanishingly small linewidths.

C. Comparison with experiments

We now look at experimentally realistic conditions. The simulation we base our discussion on is shown in Fig. 2(c). The energy of the right dot considered is $E_R = 103\mu$eV and is kept fixed. We consider the temperature of the left lead to be kept at $T_L = 2$ K, the temperature of the right lead to be kept at $T_R = 3$ K, and the temperature of the cavity to be kept at $T_H = 5T_R$. For these considerations, the stopping energy of the left dot becomes $E_L^{\text{stop}} \approx 63.4\,\mu$eV, and the optimal cooing is obtained when $E_L^{\max} \approx 31.7\,\mu$eV. The maximum cooling power obtained at the optimal bias ($E_L = E_L^{\max}$) is $Q_L^{\max} \approx 10$ eV/s. We assume a linewidth $\gamma = 10^{-4} E_R$, which approximates the results assuming a δ-function linewidth. We demonstrate in Appendix D that the asymmetric case (when $\gamma_L \neq \gamma_R$) does not cause any major changes to these predictions; for instance, the maximum cooling power is obtained still at the middle of the allowed range for the dot energies E_L even when the linewidths are not exactly identical, which is a likely scenario for the experimental implementation of our refrigerator.

V. CONCLUSIONS

We presented a new quantum absorption refrigerator scheme based on the quantum physics of resonant tunneling through quantum dots. We provided a complete thermodynamic characterization of the device and identified stopping configurations of the refrigerator where the transport is thermodynamically reversible such that Carnot COP is achieved while extracting zero cooling power. We also optimized the operation of the refrigerator with respect to externally controllable parameters for the refrigerator, such as the energy of the dots, as well as their linewidth. Our absorption refrigerator can be integrated into circuits and can offer on-chip integrable solutions to the increasing demand for cooling in the subkelvin regime, by harvesting energy from dissipating energy sources within a circuit. This is an additional benefit of our cooling scheme, which presents itself as a novel approach to recycle wasteful energy from some part of the circuit, possibly left over from a cycle of computation, for cooling other regions within the circuit. In contrast to the heat-engine mode [35], the absorption refrigerator requires a smaller linewidth.

Our present analysis has ignored many-body effects that emerge with strong electron-electron interactions in the quantum dot, but if present, they can have observable consequences to electron transport, such as the Kondo effect [70–73] due to the formation of a singlet between the conduction electrons from the lead and the dot. In such cases, the Fermi surface of the lead effectively extends to the quantum dot, such that quasiparticles traverse the dot with unit probability, resulting in increased conductance [74]. At low temperatures, such quantum correlations can enhance the cooling effect by achieving unit transmission through the dots—which makes it an interesting direction of research to explore further, although beyond the scope of our present analysis.

Different alternate implementations for our absorption refrigerator are possible; for instance, one can consider several such absorption refrigerators operating in parallel to amplify the cooling effect. Such practical solutions to harvesting dissipated heat in electronic circuits are of supreme importance to various quantum-computing platforms currently available, with the potential to improve the performance of superconducting circuits, quantum-limited detectors, and charge sensors used for various quantum information-processing applications.

ACKNOWLEDGMENTS

This work was supported by the U.S. Department of Energy (DOE), Office of Science, Basic Energy Sciences (BES), under Award No. DE-SC0017890.

APPENDIX A: EXACT SOLUTION FOR μ_H

Note that Eq. (9) can be solved exactly to obtain a solution to the chemical potential of the cavity μ_H. To find the solution, we define $z = \exp(-\mu_H/k_B T_H)$ and use the short

notation $f_\alpha = f(E_\alpha - \mu_\alpha, T_\alpha)$ for $\alpha = \mathrm{L}, \mathrm{R}$. Then, Eq. (9) becomes

$$\begin{aligned}&\left(ze^{\frac{E_\mathrm{L}}{k_\mathrm{B}T_\mathrm{H}}}+1\right)^{-1}+\left(ze^{\frac{E_\mathrm{R}}{k_\mathrm{B}T_\mathrm{H}}}+1\right)^{-1}\\&\quad=f_\mathrm{L}+f_\mathrm{R}\Rightarrow\frac{ze^{\frac{E_\mathrm{L}}{k_\mathrm{B}T_\mathrm{H}}}+ze^{\frac{E_\mathrm{R}}{k_\mathrm{B}T_\mathrm{H}}}+2}{\left(ze^{\frac{E_\mathrm{L}}{k_\mathrm{B}T_\mathrm{H}}}+1\right)\left(ze^{\frac{E_\mathrm{R}}{k_\mathrm{B}T_\mathrm{H}}}+1\right)}\\&\quad=f_\mathrm{L}+f_\mathrm{R}.\end{aligned}\tag{A1}$$

It is straightforward to write this equation in the form $az^2 + bz + c = 0$, where we find

$$\begin{aligned}&a=f_\mathrm{L}+f_\mathrm{R},\quad b=(f_\mathrm{L}+f_\mathrm{R}-1)\left(e^{-\frac{E_\mathrm{L}}{k_\mathrm{B}T_\mathrm{H}}}+e^{-\frac{E_\mathrm{R}}{k_\mathrm{B}T_\mathrm{H}}}\right),\\&c=(f_\mathrm{L}+f_\mathrm{R}-2)e^{-\frac{E_\mathrm{L}+E_\mathrm{R}}{k_\mathrm{B}T_\mathrm{H}}}.\end{aligned}\tag{A2}$$

There are two solutions to this equation given by $z_\pm = (-b \pm \sqrt{b^2 - 4ac})/(2a)$. Note that we always have $b^2 > 4ac$ since $a > 0$ and $c \leqslant 0$, which ensures that the solutions $z_\pm$ are real. However, this also implies that $z_- \leqslant 0$, which therefore is an unphysical solution as it would correspond to an imaginary chemical potential. We conclude that the chemical potential of the cavity reads

$$\begin{aligned}\frac{\mu_\mathrm{H}}{k_\mathrm{B}T_\mathrm{H}}=\ln 2-\ln\Bigg\{&\left(\frac{1}{f_\mathrm{L}+f_\mathrm{R}}-1\right)\left(e^{-\frac{E_\mathrm{L}}{k_\mathrm{B}T_\mathrm{H}}}+e^{-\frac{E_\mathrm{R}}{k_\mathrm{B}T_\mathrm{H}}}\right)\\&+\Bigg[\left(\frac{1}{f_\mathrm{L}+f_\mathrm{R}}-1\right)^2\left(e^{-\frac{E_\mathrm{L}}{k_\mathrm{B}T_\mathrm{H}}}+e^{-\frac{E_\mathrm{R}}{k_\mathrm{B}T_\mathrm{H}}}\right)^2\\&+4\left(\frac{2}{f_\mathrm{L}+f_\mathrm{R}}-1\right)e^{-\frac{E_\mathrm{L}+E_\mathrm{R}}{k_\mathrm{B}T_\mathrm{H}}}\Bigg]^{1/2}\Bigg\}.\end{aligned}\tag{A3}$$

We emphasize that the above expression can be used in all situations where the narrow-linewidth limit is justified since its derivation did not require any additional approximation. In particular, even though this work focuses on the absorption refrigerator case where $\mu_\mathrm{L} = \mu_\mathrm{R} = 0$, the chemical potentials μ_L and μ_R need not be equal.

APPENDIX B: RECTIFICATION CONFIGURATION

It is interesting to note that it is possible to drive a rectified heat current even if there is no thermal bias between the two leads, $T_\mathrm{L} = T_\mathrm{R} = T$. In this case, the second law of thermodynamics reads

$$J\left(\frac{1}{T}-\frac{1}{T_\mathrm{H}}\right)\geqslant 0.\tag{B1}$$

Since $T < T_\mathrm{H}$, this imposes $J > 0$; that is, $j\Delta E > 0$. In this situation, it is the relative position of the dot energies which dictates the directions of both the particle current and the heat flow: When $E_\mathrm{L} > 0$ and $E_\mathrm{R} > 0$, we have $j > 0$ and $Q_\mathrm{L} > 0$ (electrons and heat flow from left to right) if $E_\mathrm{R} > E_\mathrm{L}$, while $Q_\mathrm{R} > 0$ and $j < 0$ (electrons and heat flow from right to left) if $E_\mathrm{R} < E_\mathrm{L}$.

Focusing on the case $j > 0$, we realize that the only condition to be satisfied by the dot energies is $\Delta E > 0$; in other words, $r_\mathrm{stop} = 1$. In the linear response regime, we find that the cooling power is given by

$$Q_\mathrm{L}=\frac{\gamma E_\mathrm{L}\Delta E}{8\hbar k_\mathrm{B}T_\mathrm{H}}\left(\frac{T_\mathrm{H}}{T}-1\right).\tag{B2}$$

For fixed E_R, it reaches a maximum when $E_\mathrm{L} = E_\mathrm{R}/2$,

$$Q_\mathrm{max}=\frac{\gamma E_\mathrm{R}^2}{32\hbar k_\mathrm{B}T_\mathrm{H}}\left(\frac{T_\mathrm{H}}{T}-1\right),\tag{B3}$$

with the COP simply given by $C = 1$.

APPENDIX C: FLAT TRANSMISSION IN THE LIMIT OF LARGE LINEWIDTH

The transmission function of a quantum dot becomes flat in the limit of large linewidth,

$$\mathcal{T}_\alpha(E)=\frac{\gamma^2}{(E-E_\alpha)^2+\gamma^2}\approx 1.\tag{C1}$$

In practice, this approximation is relevant when γ is much larger than temperature, $\gamma \gg k_\mathrm{B}T_\mathrm{H}$ here. In this situation, the particle currents read

$$\begin{aligned}j_\alpha&\approx\frac{2}{h}\int_{-\infty}^{\infty}dE\,[f(E-\mu_\alpha,T_\alpha)-f(E-\mu_\mathrm{H},T_\mathrm{H})]\\&=\frac{2}{h}(\mu_\alpha-\mu_\mathrm{H}).\end{aligned}\tag{C2}$$

The conservation law in Eq. (9) then becomes

$$j_\mathrm{L}+j_\mathrm{R}=0\Rightarrow\mu_\mathrm{H}=\frac{\mu_\mathrm{L}+\mu_\mathrm{R}}{2}.\tag{C3}$$

Hence the particle current going through the device is

$$j=j_\mathrm{L}=-j_\mathrm{R}=\frac{\mu_\mathrm{L}-\mu_\mathrm{R}}{h}.\tag{C4}$$

Furthermore, we can compute the energy currents,

$$\begin{aligned}J_\alpha&\approx\frac{2}{h}\int_{-\infty}^{\infty}dE\,E[f(E-\mu_\alpha,T_\alpha)-f(E-\mu_\mathrm{H},T_\mathrm{H})]\\&=-\frac{\pi^2k_\mathrm{B}^2}{3h}\left(T_\mathrm{H}^2-T_\alpha^2\right)+\frac{1}{h}\left(\mu_\alpha^2-\mu_\mathrm{H}^2\right).\end{aligned}\tag{C5}$$

Using the expression for μ_H in Eq. (C3), we obtain

$$J_\alpha=-\frac{\pi^2k_\mathrm{B}^2}{3h}\left(T_\mathrm{H}^2-T_\alpha^2\right)+\frac{\mu_\alpha-\mu_{\bar\alpha}}{4h}(3\mu_\alpha+\mu_{\bar\alpha}),\tag{C6}$$

where $\bar\alpha = \mathrm{R}$ if $\alpha = \mathrm{L}$, and conversely.

In this paper, we have focused on the case of an absorption refrigerator where $\mu_\mathrm{L} = \mu_\mathrm{R} = 0$. In such a situation, we find $\mu_\mathrm{H} = 0$ for $\gamma \gg k_\mathrm{B}T_\mathrm{H}$. This implies that the particle current vanishes in this limit, $j = 0$. In contrast, the energy current remains finite,

$$J_\alpha=-\frac{\pi^2k_\mathrm{B}^2}{3h}\left(T_\mathrm{H}^2-T_\alpha^2\right).\tag{C7}$$

In particular, the heat current out of the cold reservoir L is given by $Q_\mathrm{L} = J_\mathrm{L} = -\pi^2k_\mathrm{B}^2(T_\mathrm{H}^2 - T_\mathrm{L}^2)/(3h)$. Interestingly, this limiting value does not depend on the dot energies. This is natural since the Lorentzian resonances at the dots' energies are completely blurred out in the large-linewidth limit where the transmission functions become flat. Moreover, we find that

this heat current is always negative, which further substantiates our claim that refrigeration is only possible for small linewidths.

APPENDIX D: ASYMMETRIC LINEWIDTH

In the main text, we focused on the case where the linewidth $\gamma_L = \gamma_R = \gamma$. Here, we consider the case where $\gamma_L \neq \gamma_R$, and we notice that this does not add any significant changes to the predictions we make. For example, in the linear response regime, we find that the chemical potential for the cavity in the steady state reads

$$\mu_H = -\frac{\gamma_L E_L}{\gamma_L + \gamma_R}\left(\frac{T_H}{T_L} - 1\right) - \frac{\gamma_R E_R}{\gamma_L + \gamma_R}\left(\frac{T_H}{T_R} - 1\right), \quad \text{(D1)}$$

which reduces to Eq. (27) when $\gamma_L = \gamma_R$. The cooling power in this case becomes

$$Q_L = \frac{\gamma_L \gamma_R E_L}{4(\gamma_L + \gamma_R)\hbar k_B T_H}\left[E_R\left(\frac{T_H}{T_R} - 1\right) - E_L\left(\frac{T_H}{T_L} - 1\right)\right], \quad \text{(D2)}$$

which reduces to Eq. (28) when $\gamma_L = \gamma_R$. Note that the maximum cooling power is still obtained when $E_L = r_{stop}E_R/2$, and the maximum cooling power is

$$Q_L^{max} = \frac{\gamma_L \gamma_R E_R^2 \left(T_R^{-1} - T_H^{-1}\right)^2}{16(\gamma_L + \gamma_R)\hbar k_B \left(T_L^{-1} - T_H^{-1}\right)}. \quad \text{(D3)}$$

[1] V. Serreli, C.-F. Lee, E. R. Kay, and D. A. Leigh, A molecular information ratchet, Nature (London) **445**, 523 (2007).

[2] M. V. Costache and S. O. Valenzuela, Experimental spin ratchet, Science **330**, 1645 (2010).

[3] S.-Y. Hwang, J. Soo Lim, R. López, M. Lee, and D. Sánchez, Proposal for a local heating driven spin current generator, Appl. Phys. Lett. **103**, 172401 (2013).

[4] B. Sothmann, R. Sánchez, A. N. Jordan, and M. Büttiker, Rectification of thermal fluctuations in a chaotic cavity heat engine, Phys. Rev. B **85**, 205301 (2012).

[5] B. Sothmann, R. Sánchez, and A. N. Jordan, Thermoelectric energy harvesting with quantum dots, Nanotechnology **26**, 032001 (2014).

[6] R. Kosloff and A. Levy, Quantum heat engines and refrigerators: Continuous devices, Annu. Rev. Phys. Chem. **65**, 365 (2014).

[7] J. P. Pekola, Towards quantum thermodynamics in electronic circuits, Nat. Phys. **11**, 118 (2015).

[8] J. Senior, A. Gubaydullin, B. Karimi, J. T. Peltonen, J. Ankerhold, and J. P. Pekola, Heat rectification via a superconducting artificial atom, Commun. Phys. **3**, 40 (2020).

[9] R. Landauer, Uncertainty principle and minimal energy dissipation in the computer, Int. J. Theor. Phys. **21**, 283 (1982).

[10] A. Bérut, A. Arakelyan, A. Petrosyan, S. Ciliberto, R. Dillenschneider, and E. Lutz, Experimental verification of Landauer's principle linking information and thermodynamics, Nature (London) **483**, 187 (2012).

[11] R. W. Keyes and R. Landauer, Minimal energy dissipation in logic, IBM J. Res. Dev. **14**, 152 (1970).

[12] R. Landauer, Irreversibility and heat generation in the computing process, IBM J. Res. Dev. **5**, 183 (1961).

[13] Landauer's bound is a lower bound which predicts that the minimum heat generated in erasing a classical bit's worth of information is at least $k_B T \ln 2$. The bound can be saturated by implementing erasure as a thermodynamic cycle consisting of adiabatic and isothermal processes, where T is the temperature of the heat bath facilitating the isotherms [12].

[14] G. Walker, R. Fauvel, and G. Reader, Miniature refrigerators for cryogenic sensors and cold electronics, Cryogenics **29**, 841 (1989).

[15] F. Giazotto, T. T. Heikkilä, A. Luukanen, A. M. Savin, and J. P. Pekola, Opportunities for mesoscopics in thermometry and refrigeration: Physics and applications, Rev. Mod. Phys. **78**, 217 (2006).

[16] F. Pobell, *Matter and Methods at Low Temperatures* (Springer, New York, 2007), Vol. 2.

[17] L. B. Ioffe, V. B. Geshkenbein, C. Helm, and G. Blatter, Decoherence in Superconducting Quantum Bits by Phonon Radiation, Phys. Rev. Lett. **93**, 057001 (2004).

[18] Ł. Cywiński, W. M. Witzel, and S. Das Sarma, Electron Spin Dephasing due to Hyperfine Interactions with a Nuclear Spin Bath, Phys. Rev. Lett. **102**, 057601 (2009).

[19] M. Mohseni, J. S. Lundeen, K. J. Resch, and A. M. Steinberg, Experimental Application of Decoherence-Free Subspaces in an Optical Quantum-Computing Algorithm, Phys. Rev. Lett. **91**, 187903 (2003).

[20] H. Qiao, Y. P. Kandel, S. K. Manikandan, A. N. Jordan, S. Fallahi, G. C. Gardner, M. J. Manfra, and J. M. Nichol, Conditional teleportation of quantum-dot spin states, Nat. Commun. **11**, 3022 (2020).

[21] S. Das and G. Agarwal, Decoherence effects in interacting qubits under the influence of various environments, J. Phys. B: At., Mol. Opt. Phys. **42**, 205502 (2009).

[22] A. Savin, J. P. Pekola, D. Averin, and V. Semenov, Thermal budget of superconducting digital circuits at subkelvin temperatures, J. Appl. Phys. (Melville, NY) **99**, 084501 (2006).

[23] L. Vandersypen, H. Bluhm, J. Clarke, A. Dzurak, R. Ishihara, A. Morello, D. Reilly, L. Schreiber, and M. Veldhorst, Interfacing spin qubits in quantum dots and donors—hot, dense, and coherent, npj Quantum Inf. **3**, 34 (2017).

[24] J. Labaziewicz, Y. Ge, P. Antohi, D. Leibrandt, K. R. Brown, and I. L. Chuang, Suppression of Heating Rates in Cryogenic Surface-Electrode Ion Traps, Phys. Rev. Lett. **100**, 013001 (2008).

[25] M. Leivo, J. Pekola, and D. Averin, Efficient Peltier refrigeration by a pair of normal metal/insulator/superconductor junctions, Appl. Phys. Lett. **68**, 1996 (1996).

[26] J. Pekola, J. Kyynäräinen, M. Leivo, and A. Manninen, NIS chip refrigeration, Cryogenics **39**, 653 (1999).

[27] P. Solinas, R. Bosisio, and F. Giazotto, Microwave quantum refrigeration based on the Josephson effect, Phys. Rev. B **93**, 224521 (2016).

[28] F. Giazotto and M. J. Martínez-Pérez, The Josephson heat interferometer, Nature (London) **492**, 401 (2012).

[29] S. K. Manikandan, F. Giazotto, and A. N. Jordan, Superconducting Quantum Refrigerator: Breaking and Rejoining Cooper Pairs with Magnetic Field Cycles, Phys. Rev. Appl. **11**, 054034 (2019).

[30] F. Dolcini and F. Giazotto, Adiabatic magnetization of superconductors as a high-performance cooling mechanism, Phys. Rev. B **80**, 024503 (2009).

[31] A. A. Svidzinsky, Possible cooling effect in high-temperature superconductors, Phys. Rev. B **65**, 144504 (2002).

[32] M. Campisi, Fluctuation relation for quantum heat engines and refrigerators, J. Phys. A: Math. Theor. **47**, 245001 (2014).

[33] R. S. Whitney, Most Efficient Quantum Thermoelectric at Finite Power Output, Phys. Rev. Lett. **112**, 130601 (2014).

[34] H.-T. Quan, Y.-x. Liu, C.-P. Sun, and F. Nori, Quantum thermodynamic cycles and quantum heat engines, Phys. Rev. E **76**, 031105 (2007).

[35] A. N. Jordan, B. Sothmann, R. Sánchez, and M. Büttiker, Powerful and efficient energy harvester with resonant-tunneling quantum dots, Phys. Rev. B **87**, 075312 (2013).

[36] R. Sánchez, B. Sothmann, A. N. Jordan, and M. Büttiker, Correlations of heat and charge currents in quantum-dot thermoelectric engines, New J. Phys. **15**, 125001 (2013).

[37] B. Sothmann, R. Sánchez, A. N. Jordan, and M. Büttiker, Powerful energy harvester based on resonant-tunneling quantum wells, New J. Phys. **15**, 095021 (2013).

[38] G. Benenti, G. Casati, K. Saito, and R. S. Whitney, Fundamental aspects of steady-state conversion of heat to work at the nanoscale, Phys. Rep. **694**, 1 (2017).

[39] P. Srikhirin, S. Aphornratana, and S. Chungpaibulpatana, A review of absorption refrigeration technologies, Renewable Sustainable Energy Rev. **5**, 343 (2001).

[40] K. E. Herold, R. Radermacher, and S. A. Klein, *Absorption Chillers and Heat Pumps* (CRC, Boca Raton, 2016).

[41] J. Gordon and K. Ng, *Cool Thermodynamics: The Engineering and Physics of Predictive, Diagnostic and Optimization* (Cambridge International Science, Cambridge, 2000).

[42] E. Albert and S. Leo, Refrigeration, US Patent No. 1,781,541 (11 Nov. 1930).

[43] W. Gosney, *Principles of Refrigeration* (Cambridge University Press, Cambridge, 1982).

[44] A. Levy and R. Kosloff, Quantum Absorption Refrigerator, Phys. Rev. Lett. **108**, 070604 (2012).

[45] G. Maslennikov, S. Ding, R. Hablützel, J. Gan, A. Roulet, S. Nimmrichter, J. Dai, V. Scarani, and D. Matsukevich, Quantum absorption refrigerator with trapped ions, Nat. Commun. **10**, 202 (2019).

[46] J. B. Brask and N. Brunner, Small quantum absorption refrigerator in the transient regime: Time scales, enhanced cooling, and entanglement, Phys. Rev. E **92**, 062101 (2015).

[47] M. T. Mitchison, M. Huber, J. Prior, M. P. Woods, and M. B. Plenio, Realising a quantum absorption refrigerator with an atom-cavity system, Quantum Sci. Technol. **1**, 015001 (2016).

[48] G. Jaliel, R. K. Puddy, R. Sánchez, A. N. Jordan, B. Sothmann, I. Farrer, J. P. Griffiths, D. A. Ritchie, and C. G. Smith, Experimental Realization of a Quantum Dot Energy Harvester, Phys. Rev. Lett. **123**, 117701 (2019).

[49] P. A. Erdman, B. Bhandari, R. Fazio, J. P. Pekola, and F. Taddei, Absorption refrigerators based on Coulomb-coupled single-electron systems, Phys. Rev. B **98**, 045433 (2018).

[50] L. A. Correa, J. P. Palao, D. Alonso, and G. Adesso, Quantum-enhanced absorption refrigerators, Sci. Rep. **4**, 3949 (2014).

[51] M. T. Mitchison, M. P. Woods, J. Prior, and M. Huber, Coherence-assisted single-shot cooling by quantum absorption refrigerators, New J. Phys. **17**, 115013 (2015).

[52] G. Mahan and J. Sofo, The best thermoelectric, Proc. Natl. Acad. Sci. U.S.A. **93**, 7436 (1996).

[53] J. R. Prance, C. G. Smith, J. P. Griffiths, S. J. Chorley, D. Anderson, G. A. C. Jones, I. Farrer, and D. A. Ritchie, Electronic Refrigeration of a Two-Dimensional Electron Gas, Phys. Rev. Lett. **102**, 146602 (2009).

[54] F. Hartmann, P. Pfeffer, S. Höfling, M. Kamp, and L. Worschech, Voltage Fluctuation to Current Converter with Coulomb-Coupled Quantum Dots, Phys. Rev. Lett. **114**, 146805 (2015).

[55] H. Thierschmann, R. Sánchez, B. Sothmann, F. Arnold, C. Heyn, W. Hansen, H. Buhmann, and L. W. Molenkamp, Three-terminal energy harvester with coupled quantum dots, Nat. Nanotechnol. **10**, 854 (2015).

[56] R. Wang, J. Lu, C. Wang, and J.-H. Jiang, Nonlinear effects for three-terminal heat engine and refrigerator, Sci. Rep. **8**, 1 (2018).

[57] Y. Choi and A. N. Jordan, Three-terminal heat engine and refrigerator based on superlattices, Phys. E (Amsterdam) **74**, 465 (2015).

[58] H. L. Edwards, Q. Niu, G. A. Georgakis, and A. L. de Lozanne, Cryogenic cooling using tunneling structures with sharp energy features, Phys. Rev. B **52**, 5714 (1995).

[59] This is in the same spirit as the distinction between the canonical and grand canonical ensemble in statistical mechanics.

[60] R. Landauer, Spatial variation of currents and fields due to localized scatterers in metallic conduction, IBM J. Res. Dev. **1**, 223 (1957).

[61] R. Landauer, Electrical resistance of disordered one-dimensional lattices, Philos. Mag. **21**, 863 (1970).

[62] M. Büttiker, Four-Terminal Phase-Coherent Conductance, Phys. Rev. Lett. **57**, 1761 (1986).

[63] M. Büttiker, Coherent and sequential tunneling in series barriers, IBM J. Res. Dev. **32**, 63 (1988).

[64] P. W. Brouwer, Scattering approach to parametric pumping, Phys. Rev. B **58**, R10135(R) (1998).

[65] M. Moskalets and M. Büttiker, Dissipation and noise in adiabatic quantum pumps, Phys. Rev. B **66**, 035306 (2002).

[66] M. Moskalets and M. Büttiker, Floquet scattering theory of quantum pumps, Phys. Rev. B **66**, 205320 (2002).

[67] H. B. Callen, *Thermodynamics and an Introduction to Thermostatistics* (Wiley, New York, 2006).

[68] In practice, the results obtained using this approximation hold for much higher energies, typically $|E - \mu| \sim k_B T$.

[69] Reference [35] actually focuses on the electric power delivered by the device, which is proportional to the particle current analyzed here.

[70] J. Kondo, Resistance minimum in dilute magnetic alloys, Prog. Theor. Phys. **32**, 37 (1964).

[71] D. Goldhaber-Gordon, H. Shtrikman, D. Mahalu, D. Abusch-Magder, U. Meirav, and M. Kastner, Kondo effect in a single-electron transistor, Nature (London) **391**, 156 (1998).

[72] S. M. Cronenwett, T. H. Oosterkamp, and L. P. Kouwenhoven, A tunable Kondo effect in quantum dots, Science **281**, 540 (1998).

[73] O. Zarchin, M. Zaffalon, M. Heiblum, D. Mahalu, and V. Umansky, Two-electron bunching in transport through a quantum dot induced by Kondo correlations, Phys. Rev. B **77**, 241303(R) (2008).

[74] W. Van der Wiel, S. De Franceschi, T. Fujisawa, J. Elzerman, S. Tarucha, and L. Kouwenhoven, The Kondo effect in the unitary limit, Science **289**, 2105 (2000).